AIP | Applied Physics Letters

Thermomechanical strain measurements by synchrotron x-ray diffraction and data interpretation for through-silicon vias

X. Liu, P. A. Thadesar, C. L. Taylor, M. Kunz, N. Tamura et al.

Citation: Appl. Phys. Lett. **103**, 022107 (2013); doi: 10.1063/1.4813742
View online: http://dx.doi.org/10.1063/1.4813742
View Table of Contents: http://apl.aip.org/resource/1/APPLAB/v103/i2
Published by the AIP Publishing LLC.

Thermomechanical strain measurements by synchrotron x-ray diffraction and data interpretation for through-silicon vias

X. Liu,[1] P. A. Thadesar,[2] C. L. Taylor,[1] M. Kunz,[3] N. Tamura,[3] M. S. Bakir,[2] and S. K. Sitaraman[1,a)]
[1]*The George W. Woodruff School of Mechanical Engineering, Atlanta, Georgia 30332, USA*
[2]*School of Electrical and Computer Engineering, Georgia Institute of Technology, Atlanta, Georgia 30332, USA*
[3]*Advanced Light Source, Lawrence Berkeley National Laboratory, Berkeley, California 94720, USA*

(Received 1 May 2013; accepted 23 June 2013; published online 10 July 2013)

To study thermomechanical strain induced by the mismatch of coefficients of thermal expansion in through-silicon vias (TSVs) and thus provide fundamental understanding of TSV reliability, strain measurements have been performed with synchrotron x-ray diffraction (XRD). The measured strains are available as two-dimensional (2D) distribution maps, whereas the strain distributions in TSVs are three-dimensional (3D) in nature. To understand this 3D to 2D data projection process, a data interpretation method based on beam intensity averaging is proposed and validated with measurements. The proposed method is applicable to XRD strain measurements on thin as well as thick samples. © *2013 AIP Publishing LLC*. [http://dx.doi.org/10.1063/1.4813742]

Through-silicon via (TSV) is one of the key enabling technologies for three-dimensional integrated circuit (3D IC) packaging. However, TSVs have potential thermomechanical reliability challenges due to the coefficient of thermal expansion (CTE) mismatch between copper and the surrounding silicon.[1] Prior efforts in TSV stress/strain measurements for understanding these reliability challenges, include micro-Raman spectroscopy, bending beam technique, indentation, and x-ray micro-diffraction. Micro-Raman spectroscopy works on the principle of measuring the frequency shift of an impinging laser to quantify localized near surface silicon stress.[2,3] However stresses in copper cannot be measured using micro-Raman spectroscopy. The bending beam technique works on the principle of measuring the curvature of the sample to quantify the stress in silicon and copper.[4] However the measured stresses using the bending beam technique are averaged across the sample. Indentation techniques work on the principle of analyzing the residual-stress-induced normal load to measure localized stress in silicon and copper.[5] However, it is difficult to measure residual stress in the absence of a known stress-free state using the indentation techniques. Synchrotron x-ray diffraction (XRD) can measure all the stress components in a copper via and the surrounding silicon.[6] However, data interpretation is challenging for thick structures. Depth resolved x-ray diffraction techniques, such as DAXM (Differential Aperture X-ray Microscopy), could in principle be employed but data collection would be prohibitively long to map an entire sample.[7] Raster scanning the sample under a micro focused beam provides a 2D strain distribution map of the sample, whereas the strain distributions in TSVs are three-dimensional (3D) in nature. How the strain distribution along the x-ray penetration depth direction is averaged and projected is a complicated matter as it involves multiple factors, such as x-ray energy, type of materials, as well as dynamical effects. This may not be an issue for thin structures,[8,9] however, it is essential for the interpretation of measurement results of thick samples like a silicon wafer with embedded copper TSVs. This paper presents a beam intensity based averaging method with the assistance of finite-element modeling (FEM) to interpret the measured TSV 2D strain maps.

As shown in Fig. 1, 300 μm tall TSVs with 50 μm diameter copper vias at 150 μm pitch and 1 μm thick silicon dioxide liner were fabricated using a "mesh" technique.[10] To mimic their behavior in electronic packages, a 50 μm thick copper layer was kept at the bottom of the wafer to introduce bending effect during temperature excursions. Cross-section polishing was performed until 50 μm silicon remained surrounding the TSV array. The 50 μm silicon is half the distance between two neighboring TSVs. It is kept to preserve the TSV/silicon mechanical boundary condition while still small enough for synchrotron x-rays to penetrate through.

The synchrotron x-ray diffraction test was carried out on beamline 12.3.2[11] at the Advanced Light Source (ALS), Lawrence Berkeley National Laboratory (LBNL). Scans were conducted at 150 °C using a focused polychromatic x-ray beam to measure the deviatoric strain distribution, followed by hydrostatic strain measurement of the TSV sample at selected locations using monochromatic beam scans. However, due to limited information obtained from the monochromatic scans of the selected locations, only deviatoric strain distributions were analyzed for the entire TSV scanning plane. The x-ray beam was focused to a 1 micron size via a pair of elliptically bent Kirkpatrick-Baez mirrors. Laue pattern data analysis and monochromatic powder diffraction analysis were carried out using the X-ray Micro-diffraction Analysis Software (X-MAS)[12,13] to calculate all the strain components.

Fig. 2 shows the measured 2D equivalent deviatoric strain map of silicon, where two neighboring TSVs were scanned to study the interactions between them. As seen, the highly stressed regions are near the TSVs. However, as discussed before, the 2D strain maps actually represent 3D strain distributions in silicon around TSVs. Since x-rays attenuate (Fig. 3) as they penetrate through the TSV sample due to

a)Electronic mail: suresh.sitaraman@me.gatech.edu

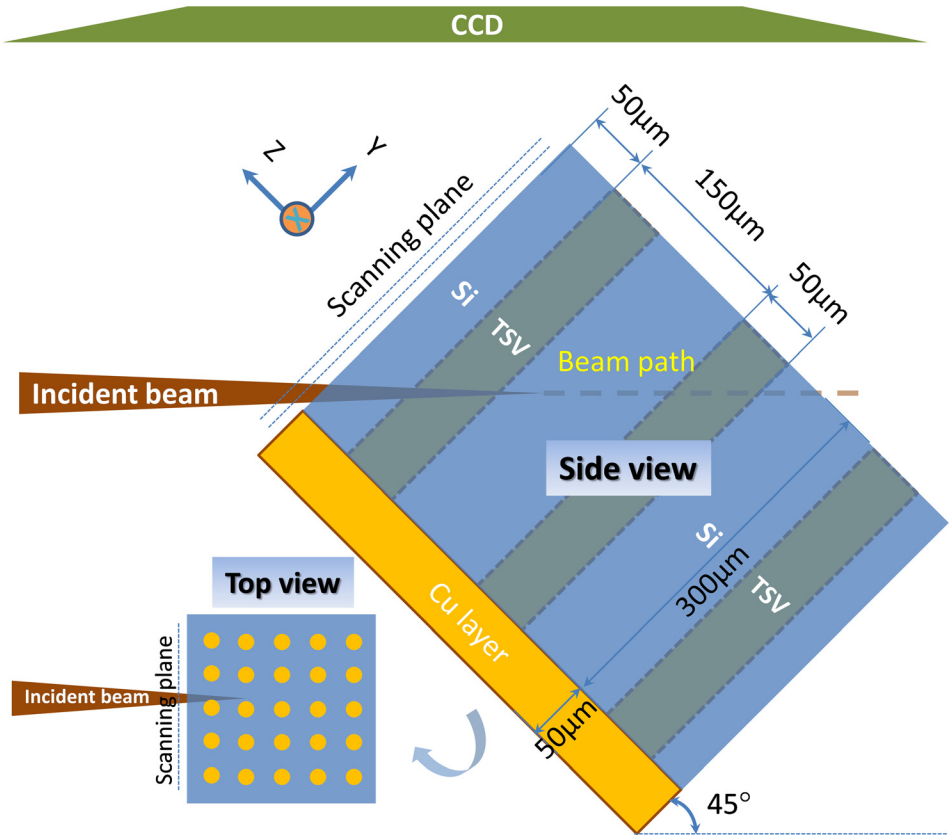

FIG. 1. TSV array sample under synchrotron x-ray diffraction test.

photoelectric absorption, scattering, and pair production,[14] the strongest signal and thus the major component of the collected information is from the front section of the TSVs. This raises two questions: how deep is the front section and how the information from the front section is represented in the 2D strain maps? The answers to these questions are essential for the interpretation of measurement results and thus understanding the TSV thermomechanical reliability.

$$\varepsilon'_{eq} = \frac{2}{3}\sqrt{\frac{(\varepsilon'_{xx}-\varepsilon'_{yy})^2+(\varepsilon'_{yy}-\varepsilon'_{zz})^2+(\varepsilon'_{zz}-\varepsilon'_{xx})^2+6(\varepsilon'_{xy}{}^2+\varepsilon'_{yz}{}^2+\varepsilon'_{xz}{}^2)}{2}} \quad (1)$$

To answer the above questions, we propose a beam intensity based data averaging method. Due to thermomechanical strain deformation in the sample, kinematical conditions apply in silicon crystals, and thus we assume that the contribution of the collected data to the final 2D strain maps depends on the distribution of the beam intensity along the beam penetration direction. In other words, since the beam intensity is higher near the front section, the strain data in this section have larger effect on the 2D strain maps, which is realized through beam intensity based weight function. The detailed data interpretation process is presented in Fig. 4. The proposed beam intensity based data averaging method calculates the intensity of the incident beam taking the white beam (5 keV to 22 keV) in 0.01 keV steps[11] as the beam passes through the TSV center lines. In this beam intensity averaging model, the flux corresponding to each energy spectrum of the white beam is taken into account using the corresponding mass attenuation coefficients. The fluxes with different energies have different penetration depths. Consequently, each flux can only be considered for a specific penetration depth and thus the hkl corresponding to their energy spectrum contribute only up to a certain depth. The penetration depth is defined as the distance from the surface to where the intensity of x-rays falls to $1/e$ of its value at the surface, where e is the Euler's number. Since the TSV

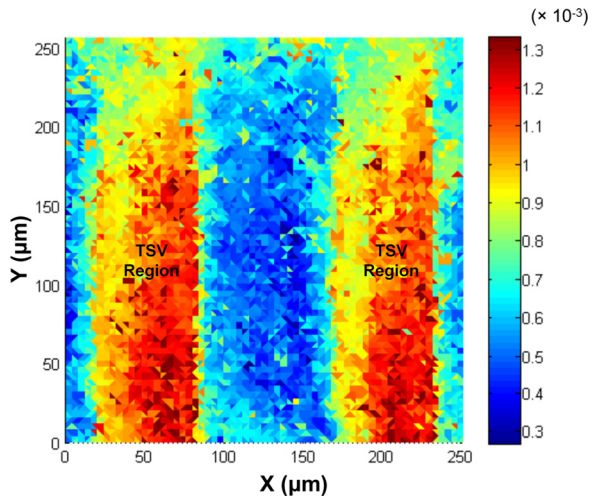

FIG. 2. Measured equivalent deviatoric strain ε'_{eq} (Eq. (1)) distribution map of silicon at 150 °C.

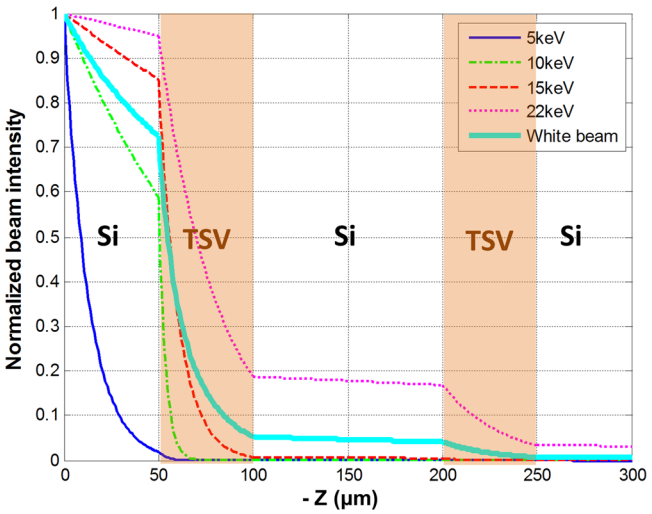

FIG. 3. Beam intensity attenuation in the TSV sample.

critical failures are mainly caused by cohesive cracks in silicon and interfacial separation between the copper and the silicon,[1] silicon was selected as the material of interest. Only the fluxes corresponding to the beam intensities in the silicon are calculated and then normalized to form the white beam intensity weight function $w(z)$, where $\sum w_i(z) = 1$. Simultaneously, a finite element TSV array model is built with the same geometry as the tested TSV sample. To capture the process-induced stress of the TSV array, the thermal profile of the fabrication process is sequentially applied to the model. To mimic the sequential fabrication process, all the materials are activated sequentially at their process stress-free temperature through the ANSYS™ element birth-and-death approach. Thereafter, the deviatoric or hydrostatic strains along the beam penetration depth direction are read out and multiplied by the beam intensity based weight function ($\varepsilon = \sum w_i \varepsilon_i$) to get a strain value at any given point on the scanning plane. This process is repeated until all the points on the scanning plane are covered. Depending on the materials along the penetration path, the penetration depth and the weight function keep changing as the beam moves in the scanning plane.

Fig. 5 shows all the measured silicon deviatoric strain components at 150 °C and the model prediction using beam

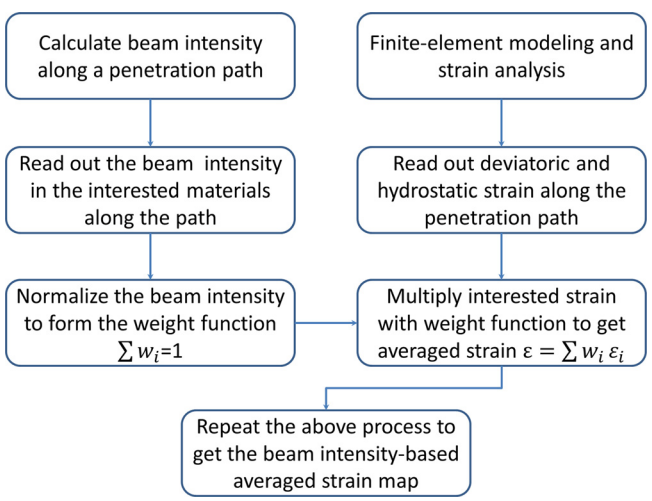

FIG. 4. Process flow of the beam intensity based data averaging method.

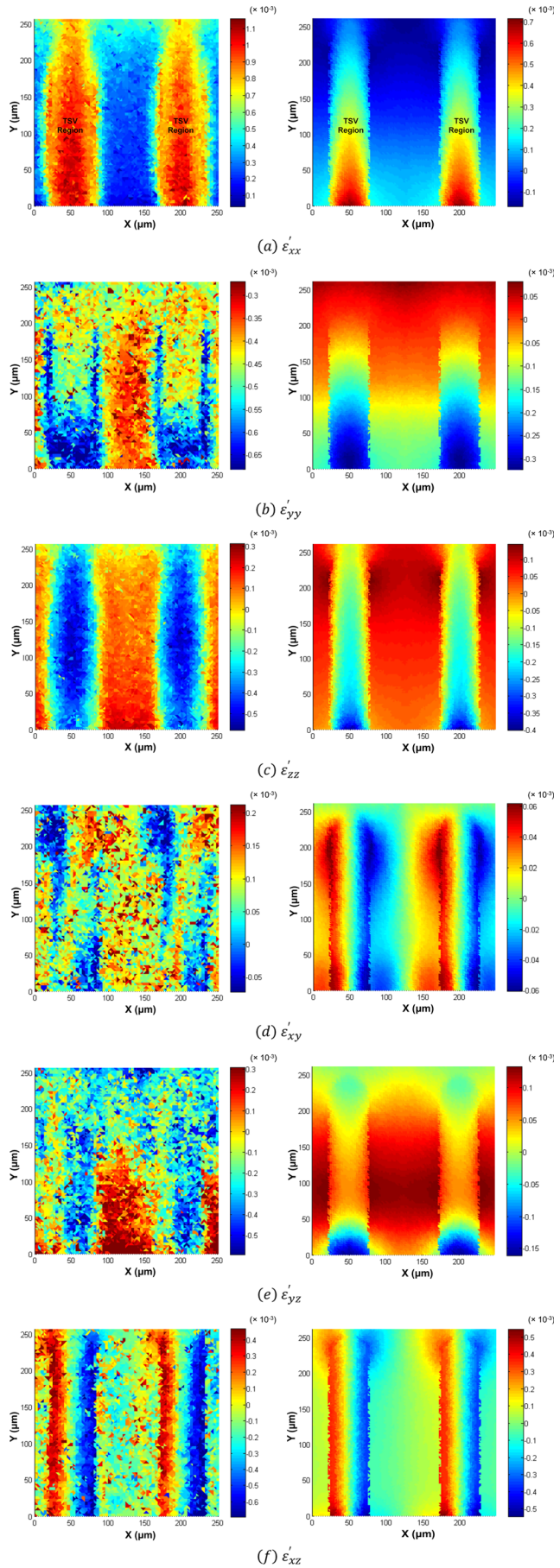

FIG. 5. Measured deviatoric strain distribution maps of silicon (left) vs. model predicted strain maps (right) at 150 °C.

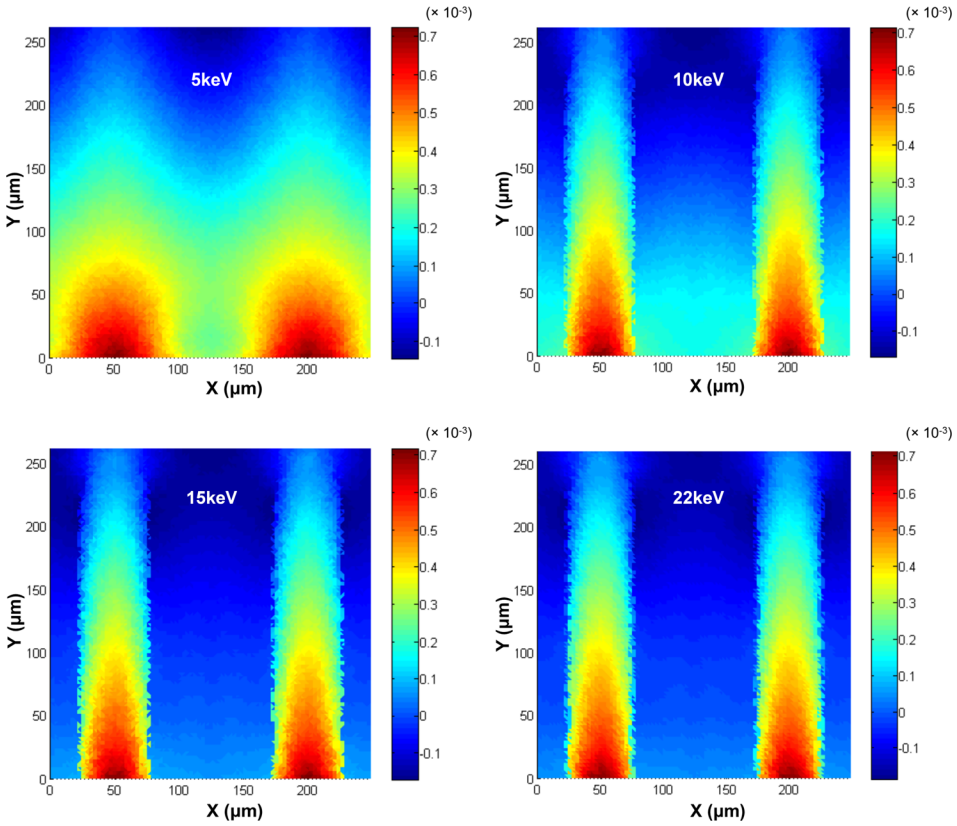

FIG. 6. Predicted ε'_{xx} distribution maps of silicon with different monochromatic beam energies.

intensity based data averaging method. The model shows that the CTE mismatch induced copper pumping at 150 °C causes large stress near the copper silicon interfaces, which is consistent with previous understandings.[1,8] The comparison shows that the model results generally agree well with the measurement data on strain distribution with some discrepancies due to various reasons. First, it was observed that while repeating the measurements on the same sample, a few measured values differed from the modeled values due to the stress history during the high temperature measurements. However, the strain distribution remained unchanged. Second, the finite element model considers an ideal thermal loading case without accounting for the fabrication induced defects and copper grain coarsening during the fabrication. Even with the discrepancies in some of the strain magnitudes, both of the modeled and measured strain distribution trends matched well for all the six components, and the trends are useful to identify critical locations in the silicon.

The above analysis with beam intensity based data averaging method used the white beam intensity for data analysis. As seen in Fig. 3, different energy spectra will result in different penetration depths and different weight function shapes. Thus, it is necessary to understand the effect of beam energy spectrum on the final results. Taking ε'_{xx} as an example, Fig. 6 shows the strain distribution using 5 keV, 10 keV, 15 keV, and 22 keV for the beam intensity based data averaging method. With energies higher than 15 keV, the predicted strain distributions stabilize, which indicates that the high energy spectrums dominate the final strain results. This also means that the final 2D strain map is a combined strain along the penetration depth instead of just near the front surface.

In addition, other possible data processing methods are investigated for comparison purpose. One method is an even average along the penetration path ($\varepsilon = mean(\varepsilon_i)$). The results show that the even averaged results change with different chosen averaging depths. Fig. 7 shows the result with full x-ray penetration depth. As seen, the even average method may be applicable to strain data interpolations for thin film type samples, but is not applicable to the data analysis of thick samples. Another method only picks the strain with the maximum absolute value along each path ($\varepsilon = sign\{\max[abs(\varepsilon_i)]\} \times \max[abs(\varepsilon_i)]$). As shown in Fig. 8, this maximum strain method also gives misleading strain distribution.

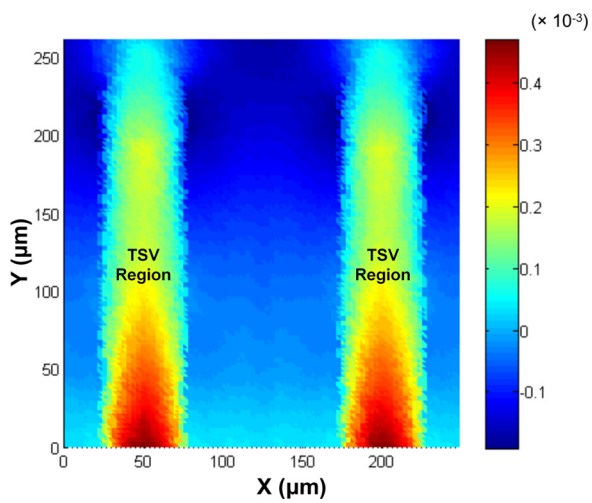

FIG. 7. Predicted ε'_{xx} distribution map of silicon with even average method.

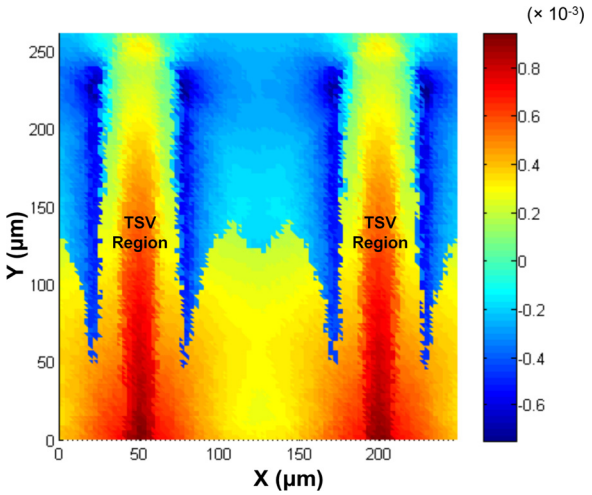

FIG. 8. Predicted ε'_{xx} distribution map of silicon with maximum strain method.

In summary, this paper proposed a beam intensity based data averaging method to interpret the synchrotron XRD measured strain data, which presents 3D strain with 2D strain maps. Results show that the proposed method successfully predicts the general trend of the strain distribution. Comparisons show that the higher energy end of the applied white beam spectrum dominates the final 2D maps. Also, the even average method and the maximum strain method may give misleading results for thick samples.

This work is supported by the Semiconductor Research Corporation under Contract No. 2012-KJ-2255. The Advanced Light Source (ALS) is supported by the Director, Office of Science, Office of Basic Energy Sciences, of the U.S. Department of Energy under Contract No. DE-AC02-05CH11231 at the Lawrence Berkeley National Laboratory (LBNL).

[1]X. Liu, Q. Chen, V. Sundaram, R. R. Tummala, and S. K. Sitaraman, Microelectron. Reliab. **53**(1), 70 (2013).
[2]I. D. Wolf, V. Simons, V. Cherman, R. Labie, B. Vandevelde, and E. Beyne, in *Proceedings of the 62nd IEEE Electronic Components and Technology Conference*, San Diego, CA, 29 May–1 June 2012, pp. 331–337.
[3]S. Ryu, Q. Zhao, M. Hecker, H. Son, K. Byun, J. Im, P. S. Ho, and R. Huang, J. Appl. Phys. **111**(6), 063513 (2012).
[4]S. Ryu, T. Jiang, K. H. Lu, J. Im, H. Son, K. Byun, R. Huang, and P. S. Ho, Appl. Phys. Lett. **100**(4), 041901 (2012).
[5]G. Lee, M. Choi, S. Jeon, K. Byun, and D. Kwon, in *Proceedings of the 62nd IEEE Electronic Components and Technology Conference*, San Diego, CA, 29 May–1 June 2012, pp. 781–786.
[6]A. S. Budiman, H. A. S. Shin, B. J. Kim, S. H. Hwang, H. Y. Son, M. S. Suh, Q. H. Chung, K. Y. Byun, N. Tamura, M. Kunz, and Y. C. Joo, Microelectron. Reliab. **52**(3), 530 (2012).
[7]B. C. Larson, W. Yang, G. E. Ice, J. D. Budai, and J. Z. Tischler, Nature **415**(6874), 887 (2002).
[8]A. S. Budiman, W. D. Nix, N. Tamura, B. C. Valek, K. Gadre, J. Maiz, R. Spolenak, and J. R. Patel, Appl. Phys. Lett. **88**(23), 233515 (2006).
[9]M. Kunz, K. Chen, N. Tamura, and H. Wenk, Am. Mineral. **94**(7), 1059 (2009).
[10]J. Lai, H. Yang, H. Chen, C. R. King, J. Zaveri, R. Ravindran, and M. S Bakir, J. Micromech. Microeng. **20**(2), 025016 (2010).
[11]M. Kunz, N. Tamura, K. Chen, A. M. Alastair, S. C. Richard, M. C. Matthew, F. Sirine, E. D. Edward, M. G. James, L. K. Jonathan, Y. M. Gregory, W. P. Dave, V. S. Brian, W. Tony, V. Y. Valeriy, A. P. Howard, and U. Ersan, Rev. Sci. Instrum. **80**(3), 035108 (2009).
[12]J. Chung and G. E. Ice, J. Appl. Phys. **86**(9), 5249 (1999).
[13]N. Tamura, A. A. MacDowell, R. Spolenak, B. C. Valek, J. C. Bravman, W. L. Brown, R. S. Celestre, H. A. Padmore, B. W. Batterman, and J. R. Patel, J. Synchrotron. Radiat. **10**(2), 137 (2003).
[14]B. D. Cullity and S. R. Stock, *Elements of X-Ray Diffraction*, 3rd ed. (Prentice Hall, Upper Saddle River, NJ, 2001).